INTERFACE

royalsocietypublishing.org/journal/rsif

Research

Cite this article: Taylor BK, Lohmann KJ, Havens LT, Lohmann CMF, Granger J. 2021 Long-distance transequatorial navigation using sequential measurements of magnetic inclination angle. *J. R. Soc. Interface* **18**: 20200887.
https://doi.org/10.1098/rsif.2020.0887

Received: 3 November 2020
Accepted: 3 December 2020

Subject Category:
Life Sciences–Engineering interface

Subject Areas:
biomimetics, biomechanics, computational biology

Keywords:
magnetoreception, magnetic reception, inclination compass, animal magnetic reception, navigation, sequential measurements

Author for correspondence:
Brian K. Taylor
e-mail: brian.taylor@unc.edu

Electronic supplementary material is available online at https://doi.org/10.6084/m9.figshare.c.5238496.

THE ROYAL SOCIETY PUBLISHING

Long-distance transequatorial navigation using sequential measurements of magnetic inclination angle

Brian K. Taylor[1], Kenneth J. Lohmann[1], Luke T. Havens[1], Catherine M. F. Lohmann[1] and Jesse Granger[2]

[1]Department of Biology, The University of North Carolina at Chapel Hill, Chapel Hill, NC, USA
[2]Department of Biology, Duke University, Durham, NC, USA

BKT, 0000-0002-0604-769X; LTH, 0000-0002-4754-2101

Diverse taxa use Earth's magnetic field in combination with other sensory modalities to accomplish navigation tasks ranging from local homing to long-distance migration across continents and ocean basins. Several animals have the ability to use the inclination or tilt of magnetic field lines as a component of a magnetic compass sense that can be used to maintain migratory headings. In addition, a few animals are able to distinguish among different inclination angles and, in effect, exploit inclination as a surrogate for latitude. Little is known, however, about the role that magnetic inclination plays in guiding long-distance migrations. In this paper, we use an agent-based modelling approach to investigate whether an artificial agent can successfully execute a series of transequatorial migrations by using sequential measurements of magnetic inclination. The agent was tested with multiple navigation strategies in both present-day and reversed magnetic fields. The findings (i) demonstrate that sequential inclination measurements can enable migrations between the northern and southern hemispheres, and (ii) demonstrate that an inclination-based strategy can tolerate a reversed magnetic field, which could be useful in the development of autonomous engineered systems that must be robust to magnetic field changes. The findings also appear to be consistent with the results of some animal navigation experiments, although whether any animal exploits a strategy of using sequential measurements of inclination remains unknown.

1. Introduction

Earth's magnetic field is a useful source of information for engineered [1,2], and biological systems ([3–5], the special edition on magnetosensing by the *Journal of the Royal Society Interface* (2010)). Extending from the crust up through the atmosphere, the magnetic field is a three-dimensional omnipresent vector signal that can be used to gain insight into both orientation, and absolute and/or relative position [1]. One way to parameterize the Earth's magnetic field is to use its inclination angle (i.e. angle from the local horizontal as defined by the direction of gravity), direction of magnetic North (i.e. the reading a compass would give) and field intensity (i.e. also known as field strength) [6,7]. Figure 1 provides several illustrations of the magnetic field.

In autonomous engineered systems, magnetic field information can be useful in a variety of navigation applications, including situations where GPS signals are unavailable or unreliable, and scenarios where other sensory modalities are compromised [1,2,8]. In biological systems, magnetic reception appears to be a sensory modality that, alongside other sensory cues, helps several animals achieve remarkable feats that parallel the goals of engineered systems (e.g. sea turtles migrating across oceans [9–11], insects navigating on the scale of continents [12,13], and birds in transcontinental migrations [14–17]). However, magnetic reception and its interaction with other sensing modalities remains poorly understood (e.g. the special edition on magnetic reception by the *Journal of the Royal*

© 2021 The Author(s) Published by the Royal Society. All rights reserved.

Downloaded from http://royalsocietypublishing.org/rsif/article-pdf/doi/10.1098/rsif.2020.0887/923617/rsif.2020.0887.pdf
by UNC Chapel Hill user
on 17 June 2026

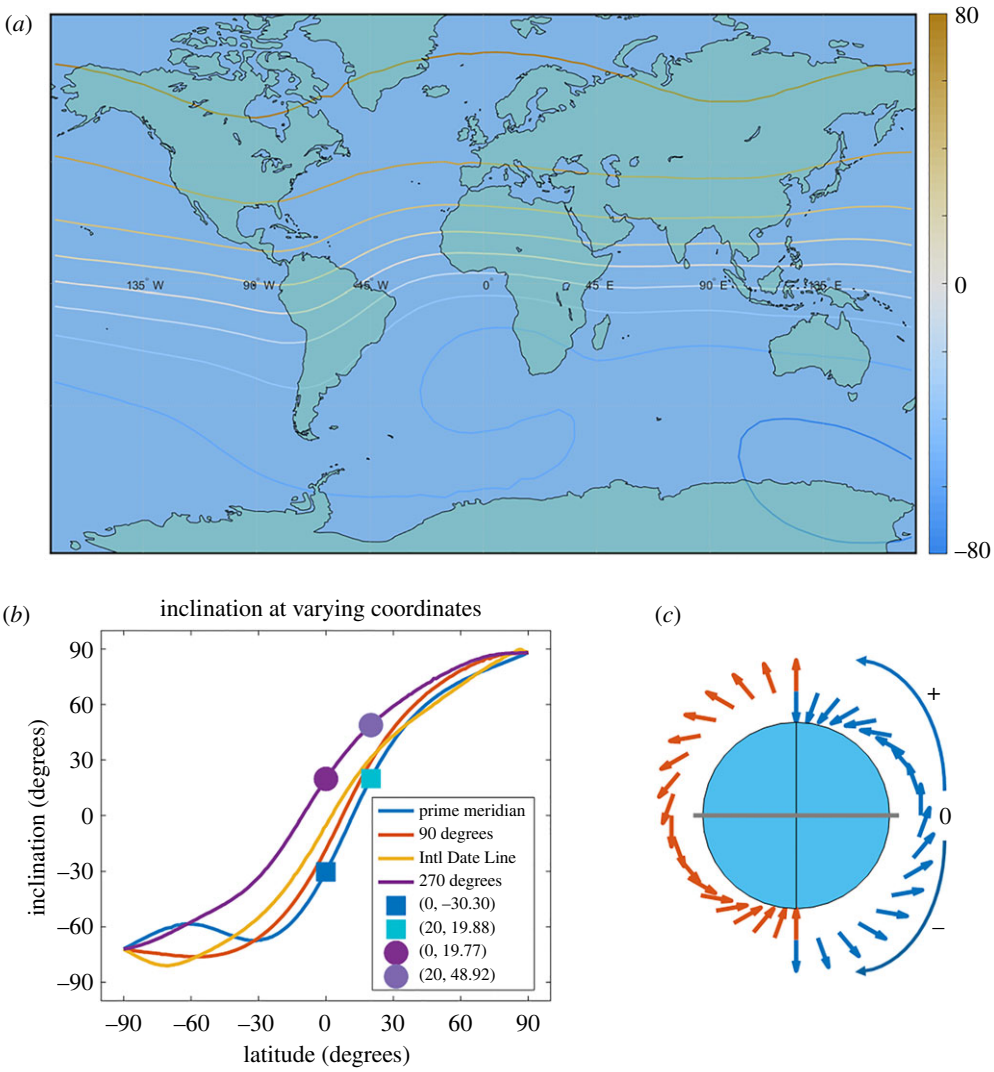

Figure 1. (*a*) Map of constant lines of inclination across the world. As can be seen, inclination generally increases from the Southern Hemisphere towards the Northern Hemisphere. (*b*) Illustration of the magnetic inclination from the South Pole (−90° latitude) to the North Pole (90° latitude) for the prime meridian, and meridians that are 90°, 180° (International Date Line), and 270° from the prime meridian. As can be seen, for all four meridians, the inclination angle generally increases from the South Pole to the North Pole. (*c*) Illustration of a present-day field (blue arrows on the right) versus a reversed field (orange arrows on the left). The curved arrows on the right show that in the present-day field, the inclination angle increases as one moves north, and decreases as one move south. Data for (*a*) and (*b*) taken from National Oceanographic and Atmospheric Administrations' (NOAA's) Enhanced Magnetic Model (EMM) (https://www.ndgc.noaa.gov/geomag/geomag.shtml).

Society Interface (2010), [5,18,19]). While laboratory animal behaviour experiments are a powerful tool, their limitations prevent them from showing the full context and scope of an animal's behaviour (e.g. [20]). Additionally, the sensory mechanisms of magnetoreception are still not conclusively known [21–28], so connecting behaviour to its sensory underpinnings is difficult.

Mathematical modelling of magnetoreceptive behaviour is an attractive complementary research tool because it allows aspects of a behaviour or environment that are difficult to examine in a laboratory or field setting (e.g. temporal shifts that happen over the course of thousands of years) to be implemented and experimentally manipulated in a simulation or model [29,30]. Some works have focused on theoretical moment-to-moment (i.e. sequential) modelling approaches that would account for detailed decision-making along a trajectory [31–35]. Others have examined the ecological impacts of high-level navigation behaviours, such as actively swimming at specific locations or waypoints along a migratory route versus passively drifting the rest of the time [20,29,30,36,37]. Results from these types of studies can generate hypotheses and insights about how a behaviour is executed. These hypotheses and insights can be compared to, reconciled with, and used to help guide real-world animal behaviour experiments to shed light on how a given behaviour is generated and performed. Such work has led to advances in both engineered system development and biological understanding in a variety of other areas (e.g. [38–44]).

Animals are known to use magnetic information in several different ways. Many exploit the geomagnetic field as a source of directional or compass information for maintaining consistent headings. Two functionally different magnetic compass types exist in animals; one type uses the inclination of field lines in combination with gravity to determine a direction of travel [14–17], while the other type uses the polarity or direction of the field (e.g. [45]). In addition, a few species of animals derive positional or map information from the geomagnetic field by sensing a combination of magnetic features such as inclination and intensity [10].

Diverse animals, including fishes, birds and mammals, undertake transequatorial migrations [15,17,46–51]. In principle, because magnetic inclination varies from −90° at the

Downloaded from http://royalsocietypublishing.org/rsif/article-pdf/doi/10.1098/rsif.2020.0887/923617/rsif.2020.0887.pdf
by UNC Chapel Hill user
on 17 June 2026

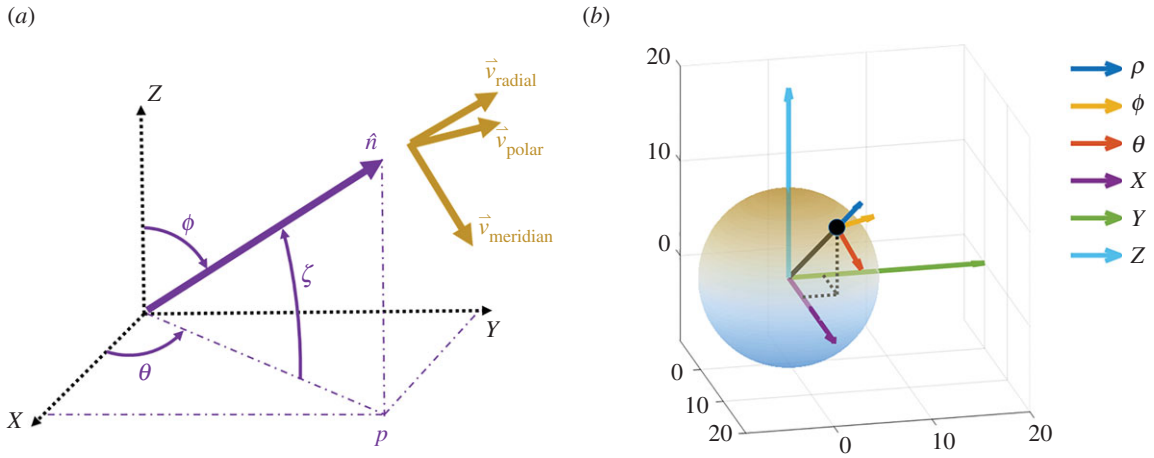

Figure 2. Illustration of the spherical coordinate system used in this study. (*a*) Definitions of all vectors and associated angles. ϕ and θ are the depression, and polar angles, respectively. The vector triad in gold is the frame in which velocities are defined. (*b*) Illustration of the final spherical coordinate frame relative to the fixed *XYZ* frame.

South Pole to 90° at the North Pole, this parameter might provide a signal that an animal could use to determine whether it is in the Northern or Southern Hemisphere. In addition, because inclination varies predictably across the Earth's surface, it might be used to guide movements across long distances if migratory animals monitor inclination as they travel. Little is known, however, about how long-distance magnetic navigation strategies are organized. An additional question that has been difficult to resolve is how navigational strategies based on magnetic fields might be affected by the reversals in Earth's field that periodically occur [6,52,53].

This paper explores possible strategies for using magnetic inclination to execute transequatorial migrations via an agent-based simulation. Specifically, we explore (i) different strategy implementations that use sequential measurements of magnetic inclination, and their ability to execute a transequatorial migration, (ii) whether a proposed method would be tolerant of a magnetic field reversal, and (iii) the implications of a strategy on the required sensitivity of any potential underlying sensory mechanisms. We emphasize that there is no experimental evidence to suggest that animals do or do not use sequential measurements of inclination to determine a direction of travel, and our presentation is not intended to say that they do. However, the results appear consistent with some previous animal experiments, illustrate the sensitivity that might be required for navigation based on inclination angle, and could be useful for developing autonomous engineered systems that are tolerant of changes in the magnetic field.

2. Methods

We implement two strategies for executing multiple transequatorial migrations. To test these strategies, we have an artificial agent (representative of an animal or engineered autonomous vehicle) begin at one location and then attempt to complete several transequatorial migrations. Two of these migrations are in a magnetic field that resembles the present-day field, while the other two are in reversed magnetic fields. This allows us to ascertain whether a given strategy can execute a transequatorial migration, and whether it can tolerate a field reversal. The migrations are intended to mimic the seasonal migrations of birds in which a full migration loop might consist of migrating from north to south, then south to north. This section first describes the agent's motion model, followed by the implementation of the magnetic field. It then outlines two magnetic field navigation strategies. It concludes with an outline of our experiments, and an analysis that examines the viability of the strategies. We emphasize that this is a conceptual study, and *only* focuses on whether a strategy can execute a migration across the Equator. It is *not* concerned with identifying a specified target location. This section states only high-level concepts, and mathematics where necessary. Detailed mathematics are presented in appendix A.

2.1. Motion model

Our agent's motion model is kinematic, and based on forming velocities in spherical coordinates ([54], and figure 2). This is done to mimic moving around a globe without the complexity of implementing an oblate spheroid model [55]. The coordinates for our system are radial distance (ρ), and depression (i.e. motion along a specific meridian—similar to latitude) (ϕ) and polar/azimuthal direction about the north–south axis (similar to longitude) (θ) (figure 2). Note that ρ is a length, while ϕ and θ are angles. Here and throughout the rest of the paper, a dot represents the time derivative of a quantity (e.g. $\dot{\phi} = \mathrm{d}\phi/\mathrm{d}t$).

Qualitatively, the agent's velocity is specified in a spherical coordinate frame that changes orientation based on spatial location (figure 2*b*). To compute the agent's position, the spherical coordinate velocity is first expressed in a fixed *XYZ* coordinate system, and then numerically integrated via Euler steps (see appendix A(a) for mathematical details).

A spherical coordinate approach was chosen for ease of implementation, though it has several drawbacks. Notably, it cannot easily cross the poles due to singularities, so moving directly past $\phi = 0$ or 180 can generate counterintuitive trajectories. An approach that uses a method such as quaternions would be more robust [55]. However, the spherical coordinate approach is simpler to implement and was deemed acceptable for initial concept exploration.

2.2. Magnetic field

We model the magnetic field as a vector field with unit magnitude at every point. Although the real magnetic field has a magnitude that varies with space (i.e. magnetic intensity, see figure 1), because this study is only concerned with inclination angle, a unit magnitude eases implementation. The direction of the field is based on figure 1, which shows that the inclination of the field mostly increases as one moves from the South Pole to the North Pole (i.e. −90° to 90°). Even in the case of the prime meridian, the inclination monotonically increases from

Downloaded from http://royalsocietypublishing.org/rsif/article-pdf/doi/10.1098/rsif.2020.0887/923617/rsif.2020.0887.pdf
by UNC Chapel Hill user
on 17 June 2026

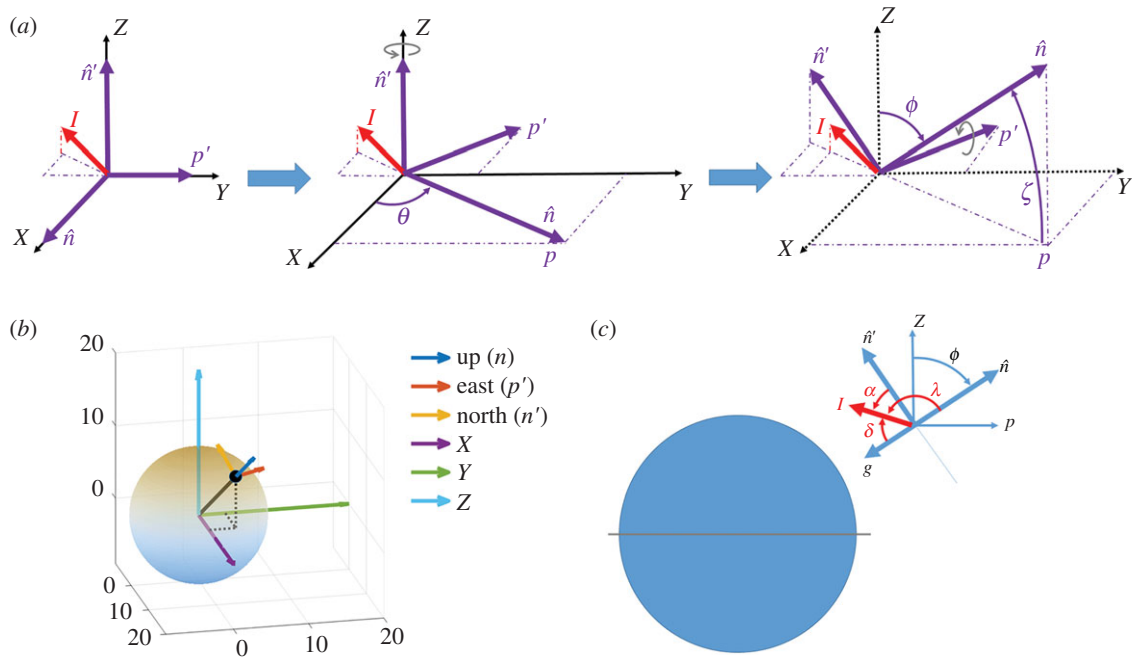

Figure 3. (*a*) Illustration of the 3D coordinate system used to define the magnetic field vector. The $\hat{n}p'\hat{n}'$ is first rotated by θ about the *Z*-axis. It is then rotated by ζ about the p' axis. Note that θ is the same as in spherical coordinates, and ζ is related to the spherical coordinate depression angle by $\phi = \zeta - 90°$. The resulting frame resembles an east-north-up frame. (*b*) Illustration of the final $\hat{n}p'\hat{n}'$ frame relative to a fixed *XYZ* frame on a sphere. (*c*) Illustration of the ways in which inclination angle can be defined.

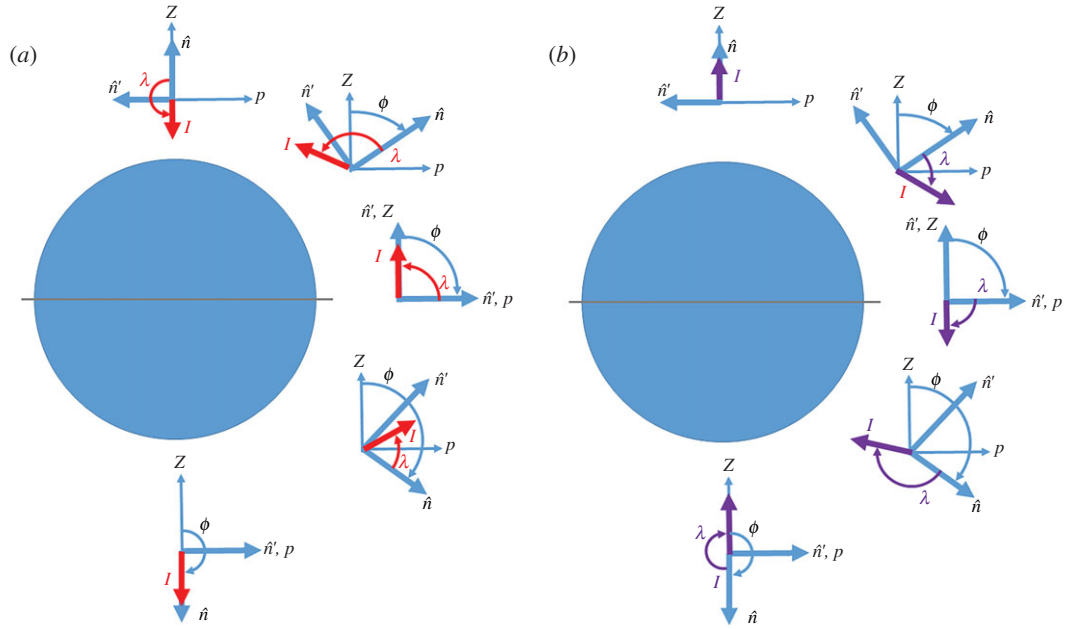

Figure 4. (*a*) Illustration of inclination angle around the world in a present-day field. (*b*) Illustration of inclination angle around the world in a reversed magnetic field.

about −30° latitude all the way to the North Pole (90°). Therefore, we model the magnetic inclination as a linear function whose inclination is −90 at the South Pole, 0 at the geometric equator, and 90 at the North Pole. In reality, the magnetic and geometric equators do not necessarily coincide, and as figure 1*c* shows, inclination is really a sigmoidal function of latitude. However, as figure 1*c* shows, inclination is linear over a large swath of latitudes. Furthermore, the strategies that we present are only concerned with whether an inclination measurement increases or decreases with agent motion, not specific numerical values. Lastly, as will be seen in §§2.5 and 3, our model has a shallower inclination slope over the central latitudes than the real world magnetic field. This means that across the Equator, our model would be more difficult to navigate than the real world because the inclination changes more slowly with north/south motion.

Qualitatively, we specify the magnetic field vector relative to a coordinate system that resembles an *east-north-up* frame [55]. Similar to a spherical frame, this coordinate system changes orientation based on location. The field vectors can be defined using figures 3 and 4.

It is convenient to define the magnetic field vector's angle (referred to as λ) from the unit vector $\hat{n}$. The standard definition of inclination (referred to as α) measures inclination angle from the unit vector $\hat{n}'$. Putting all of this together and noting the

Downloaded from http://royalsocietypublishing.org/rsif/article-pdf/doi/10.1098/rsif.2020.0887/923617/rsif.2020.0887.pdf
by UNC Chapel Hill user
on 17 June 2026

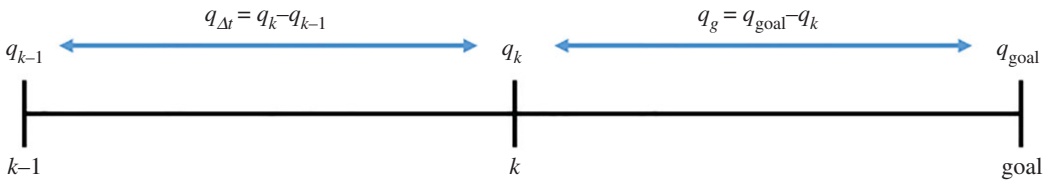

Figure 5. Illustration of a sequentially changing property.

geometry of figure 3, we can make the following definitions for the inclination angle and magnetic field vector. Note that these angles and vectors are given relative to the $\hat{n} - \hat{p}' - \hat{n}'$ frame.

$$\vec{I}_n = \begin{bmatrix} \cos(\lambda) \\ 0 \\ -\sin(\lambda) \end{bmatrix}. \tag{2.1}$$

To make the inclination angle λ a linear function of the depression angle ϕ, we use the point slope formula

$$\lambda = \left(\frac{\lambda_2 - \lambda_1}{\phi_2 - \phi_1}\right)(\phi - \phi_1) + \lambda_1. \tag{2.2}$$

Figure 4 shows various magnetic field inclination angles relative to their associated depression angles in both present day, and reversed magnetic fields. In the present-day, the field points out of the Earth in the Southern Hemisphere and into the Earth in the Northern Hemisphere, with magnetic flux lines exiting the South Pole and re-entering the North Pole (figure 1*d*, blue arrows). When the field is reversed, it points out of the Earth in the Northern Hemisphere, and into the Earth in the Southern Hemisphere, with magnetic flux lines exiting from the North Pole and reentering at the South Pole (figure 1*d*, purple arrows). Regardless of whether values for *either* the regular or reversed field are selected, the slope term in equation (2.2) is positive, *which makes our proposed strategies possible*.

By selecting two points in either figure 4*a* or *b*, and substituting the associated values into equation (2.2) we can construct the magnetic field vector relative to the $\hat{n} - \hat{p}' - \hat{n}'$ frame. To relate the standard definition of inclination α to λ, we can again use the point slope formula with α and λ at two separate latitudes (see appendix A(b)).

2.3. Sequential strategies

These strategies operate by assuming that sequential measurements of the inclination or one of its related properties (figures 3 and 4) should continually increase or decrease as one makes progress towards a goal latitude.

To provide context, figure 5 illustrates a quantity q at three locations: the current time step (k), the previous time step ($k-1$) and the goal (goal). Defining $q_{\Delta t} = q_k - q_{k-1}$, and $q_g = q_{\text{goal}} - q_k$, one can see that if $q_{\Delta t}$ and q_g have the same sign, then all three points are in order (i.e. ascending or descending from $k-1$ to goal). If the signs of these terms are not equal, then the terms are not in order. If an agent wishes to travel to goal, it can determine if it is moving in the correct direction by determining if the signs of these two quantities are the same. If they are, then it can continue moving in the same direction. If they are different, then its commanded direction must be reversed. In the case of moving along a meridian (i.e. the focus of this study), this is accomplished by reversing the sign of the turn rate $\dot{\phi}$.

2.3.1. Sequential inclination

This strategy assumes that the simulated agent is capable of *directly* measuring the magnetic inclination *as it is typically defined* (i.e. α in figure 3*c*). If the magnetic field structure coincides with the present magnetic field (i.e. pointing towards the Earth in the Northern Hemisphere, and out of it in the Southern Hemisphere), then one could migrate north by moving in a direction that continually increases the measured inclination angle. Presumably, an animal would know what direction to travel based on numerous factors such as the goal location's properties (e.g. magnetic inclination, temperature, food availability), learning from other conspecifics, and previous experience. Using the notation of figure 5, and replacing q with the inclination angle α, if the sign of α_g does not match the sign of $\alpha_{\Delta t}$, then the turn rate ($\dot{\phi}$) of the agent is reversed. Otherwise, it stays the same.

Table 1. Goal angles and locations for the agent. Angular distances are in degrees, and transnational distances are in metres.

	ϕ	θ	x	y	z
1	170	0	1.7365	0	−9.8481
2	10	90	0	1.7365	9.8481
3	170	180	−1.7365	0	−9.8481
4	10	270	0	−1.7365	9.8481

2.3.2. Sequential inclination complement

This strategy directly compares the magnetic field with the gravity vector. Mathematically, this can be accomplished through the dot (i.e. scalar) product, which gives a mathematical way of obtaining the cosine of the angle between two vectors via the following:

$$\|\vec{I}\|\|\vec{g}\|\cos(\beta) = \vec{I} \bullet \vec{g}, \tag{2.3}$$

where $\|\square\|$ is the vector magnitude, $\vec{I}$ is the magnetic field vector and $\vec{g}$ is the gravity vector. This may be plausible because cosine weighting occurs in many biological sensing phenomena [56]. We use unit vectors for $\vec{I}$ and $\vec{g}$ because we are only concerned with vector directions, so the magnitudes in equation (2.3) are unity.

We compute three dot products: (i) the dot product between the goal inclination vector and gravity (δ_{goal}), (ii) the dot product between the current inclination vector and gravity (δ_k) and (iii) the dot product between the inclination vector at the previous time and gravity (δ_{k-1}), where k again represents the time step. Again, using the notation of figure 5, and replacing q with δ, if the sign of $\delta_{\Delta t}$ equals that of δ_g, then the agent is moving in the correct direction. Otherwise, it reverses the sign of its turn rate (i.e. $\dot{\phi}$).

2.4. Experiments

We investigated whether the described strategies are capable of executing transequatorial migrations in both present-day and reversed magnetic fields. For each strategy, the agent seeks four-goal depression angles (ϕ) at different values of azimuthal angle (θ). This results in two round-trip migrations that consist of a total of four migration legs: geographical north-to-south and south-to-north migrations in a present-day field, and geographical north-to-south and south-to-north migrations in a reversed field. The goal depression angles and corresponding xyz locations are given in table 1.

To ease visualization, each migration is plotted on a different meridian of a sphere. ρ is set to 10 m for all experiments. The final

Downloaded from http://royalsocietypublishing.org/rsif/article-pdf/doi/10.1098/rsif.2020.0887/923617/rsif.2020.0887.pdf
by UNC Chapel Hill user
on 17 June 2026

values of ϕ and $\dot{\phi}$ for a given migration are used as the initial value of ϕ and $\dot{\phi}$ in the next migration. Δt is set to 0.1s. The initial depression angle for the simulation is $\phi = 10°$.

Two general scenarios were run: a deterministic scenario to verify whether the strategies were capable of transequatorial migration under ideal circumstances, and a stochastic scenario where noise was injected into the polar and meridian velocities, and measurements were taken at a prescribed frequency. We injected noise to examine the robustness of the strategies under non-ideal movement conditions. Each scenario is described in the following subsections.

2.4.1. Deterministic

In this scenario, $\dot{\rho} = \dot{\theta} = 0$ (i.e. no polar or radial velocity). The magnitude of $\dot{\phi}$ is set to $10° \text{ s}^{-1}$, with the sign being determined by the given strategy. In this way, the agent *only* moves north/south along a given meridian at the prescribed angular velocity. Additionally, in this scenario, magnetic measurements are computed at every time step, and success is declared if the agent moves within 0.5 m of the goal. It is possible to look for a goal location in the deterministic scenario because the agent starts and ends on the same meridian and altitude as the goal point, so searching for a goal location is akin to searching for a goal depression angle. This is not the case in the stochastic scenario.

2.4.2. Stochastic

In the stochastic scenario, several additional factors are included. First, magnetic measurements were only taken every 10 time steps, which simulates an animal only checking in with the field every so often [13,45], or an engineered system that has a prescribed measurement frequency. Second, noise was added to both the polar and meridian velocities (i.e. $\dot{\theta}$ and $\dot{\phi}$, respectively). The polar velocity was modified such that

$$\dot{\theta}_k = \zeta, \tag{2.4}$$

where ζ is a random number drawn from a zero mean normally distributed random distribution with variance σ_ζ^2. For this study, $\sigma_\zeta = 20°$.

The meridian velocity $\dot{\phi}_k$ was modified such that when a measurement was taken, the agent moved in the correct direction for a period of time before becoming corrupted by noise. This effectively allowed the agent to start moving in the correct direction, while forcing its meridian motion to eventually turn into a biased random walk (see appendix A(c) for mathematical details).

In this scenario, the agent declared success if it moved within 3° of the goal depression angle. We had the agent seek a goal depression angle instead of a goal location in the stochastic case because nothing in the agent's strategy was designed to locate a specific target. The strategies only executed general north–south transequatorial motion. In both the deterministic and stochastic case, the software computed the ideal travel time with no noise, then gave the agent four times this amount of time to complete the migration. While this amount of time is arbitrary, four times the ideal travel time represents two round trip migrations. It was felt that if the agent was unable to complete the task within this time period, then it would take an excessively long time to accomplish the task and should be considered a failure.

2.5. Analysis

To put our results in a real-world context, we examine the sensitivity of inclination to latitude for the real geomagnetic field between the Equator (0°), and 20° of latitude for both the prime meridian, and meridian 270° from the prime meridian (circles and squares in figure 1*c*). These meridians were chosen because they represent steep (prime meridian), and shallow (270°) inclinations with respect to latitude. Zero degrees and 20° of latitude were used because these represent areas where the inclination appears to be linear with latitude, which facilitated the analysis (i.e. directly measuring slopes versus numerically approximating derivatives). To examine the sensitivity, we compute the slope of the inclination with respect to latitude for both meridians. These slopes physically represent how much the inclination angle changes for each degree of latitude change. We then compute how much the inclination would change for 1°, 0.5° and 0.25° of arc along a meridian, along with the linear distance spanned by each one of these latitude increments. For this analysis, we assume that the Earth is a sphere, and use the semi-major axis of the Earth as an approximation for its radius (given by [55]) as 6378 km. While this assumption is not truly correct (Earth is an oblate spheroid [55]), it simplifies the analysis while realistically framing our results.

3. Results

Figure 6*a*,*b* shows deterministic trajectories for each of the strategies presented in appendix A(b). As can be seen, the sequential inclination and sequential inclination complement strategies are both capable of autonomous transequatorial migrations in both present-day, and reversed magnetic fields.

Figure 6*c*,*d* shows trajectories from trials with noise introduced in both the polar and meridian directions. As can be seen, even with noise present, both strategies are capable of successfully completing transequatorial migrations in both present-day and reversed fields. To ensure that success in the stochastic case was not by chance, both strategies were run 1000 times. The strategy was able to reach all four goal depression angles in 914 of these 1000 trials (91.4%). We note that it is possible that the cases that failed may succeed if given enough time, though the completion time might be unacceptable from an ecological or engineered standpoint. The analysis results that place the work in a real-world context are shown in figure 7.

4. Conclusion and discussion

Our results demonstrate that using magnetic inclination in a sequential manner provides a viable approach for successfully executing a transequatorial migration. In particular, the findings (i) appear consistent with previous animal experimental data [15–17], and (ii) concretely demonstrate that an inclination-based directional navigation system could be robust to magnetic field reversals, further solidifying claims regarding the robustness of using inclination as a navigation cue [16]. In addition, our findings show that an inclination-based strategy may be within the capability of an animal's magnetoreceptive sensitivity. Although no animal's inclination sensitivity is conclusively known, [57] gives a worst-case inclination sensitivity for newts between 0.5° and 2°, and some findings suggest considerably greater sensitivity in animals [58,59]. Figure 7 shows that this type of sensitivity would allow our strategy to sense distances within a quarter to 1° of latitude. Even if an animal has a level of sensitivity that makes locating a particular latitude unfeasible, comparing inclination changes over time, and to that of the desired goal could still help assess gross distance travelled along a route.

Interestingly, even if we adopt conservative estimates for inclination angle sensitivity, the model would still function adequately for many species of migratory birds, which travel at airspeeds between 11.0 m s^{-1} and 20.6 m s^{-1} [60]. At these

Downloaded from http://royalsocietypublishing.org/rsif/article-pdf/doi/10.1098/rsif.2020.0887/923617/rsif.2020.0887.pdf
by UNC Chapel Hill user
on 17 June 2026

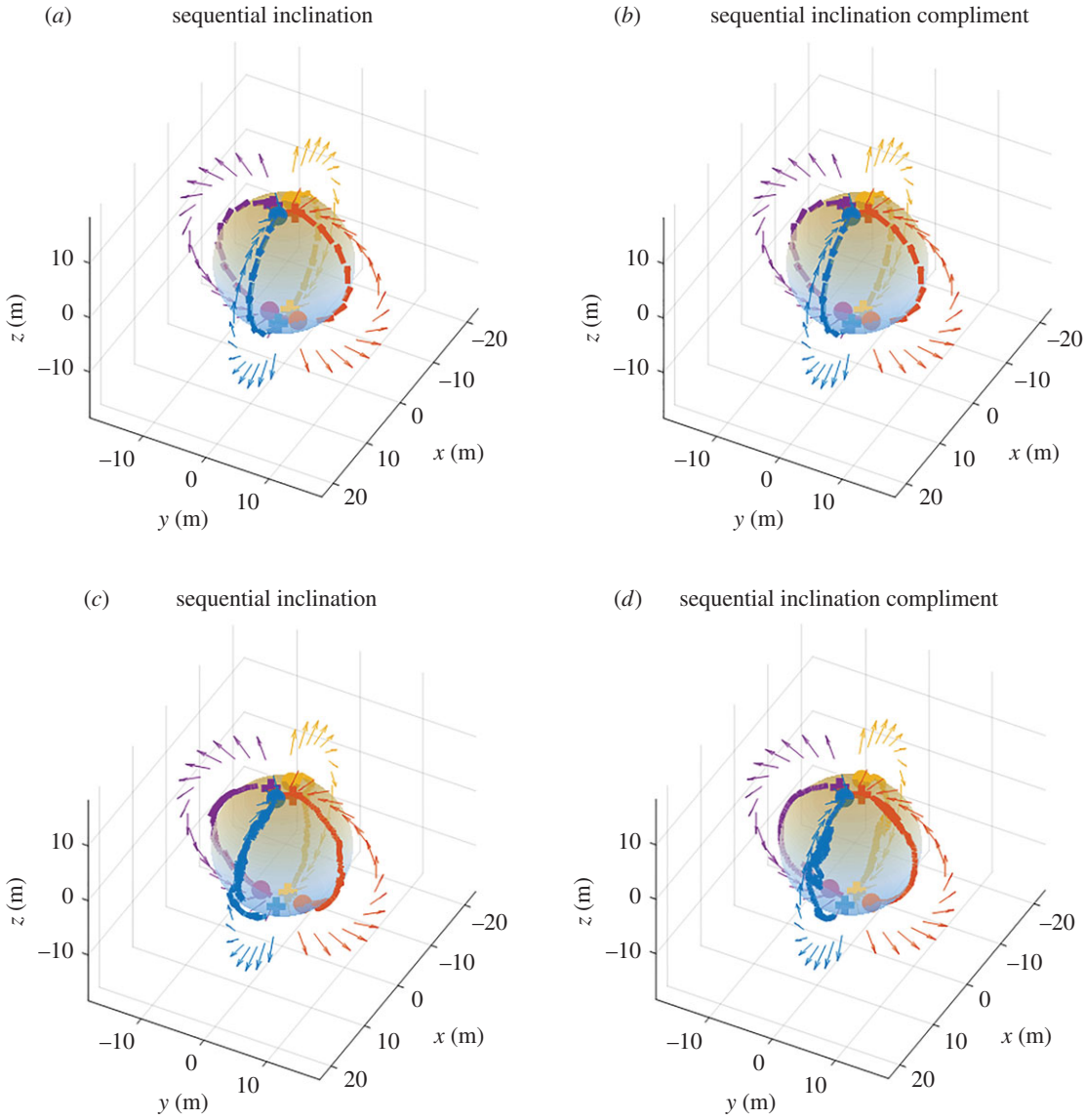

Figure 6. Trajectories from several migrations for the deterministic (*a*,*b*), and stochastic (*c*,*d*) scenarios. In (*a*,*b*), the thick arrows show the agent's direction of travel for each migration. In (*c*,*d*), the thick lines show the agent's path for each migration. The agent moves from a dot to a cross of the same colour.

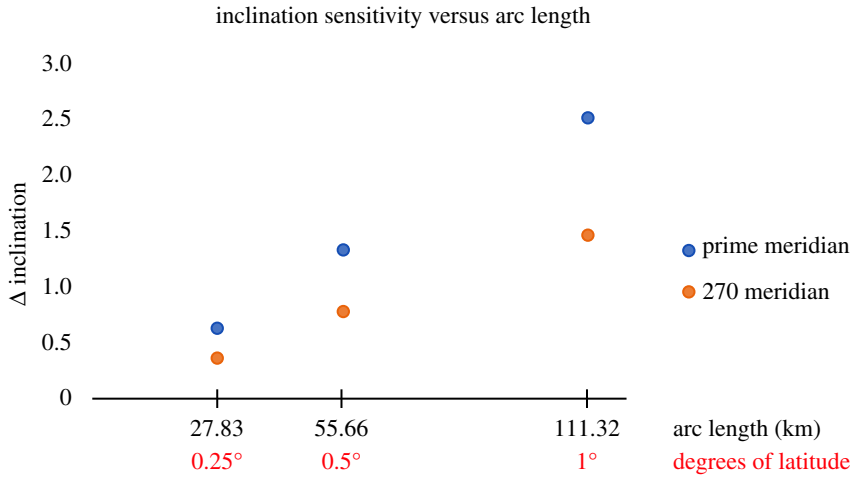

Figure 7. Sensitivity analysis demonstrating the inclination sensitivity required to sense a given change in latitude at both the prime meridian (dark blue dots), and 270° meridian (bright orange dots). Both trends are linear.

speeds, and with an assumed inclination sensitivity that would enable sensing 1° of latitude change (rightmost points in figure 7), it would take between 90 min and 168 min for an animal to sense a change in the inclination angle (arc length/flight speed). If the sensitivity is higher, then shorter flight durations will lead to detectable inclination changes. In the context of migratory routes that are thousands of kilometres long and travelled over the course of weeks to months [61], such

Downloaded from http://royalsocietypublishing.org/rsif/article-pdf/doi/10.1098/rsif.2020.0887/923617/rsif.2020.0887.pdf
by UNC Chapel Hill user
on 17 June 2026

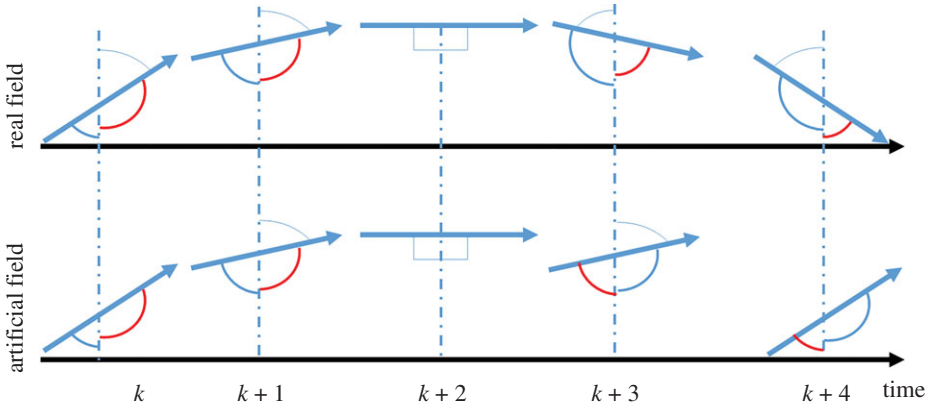

Figure 8. Illustration of tracking a magnetic field vector that continually changes in one direction. Red lines denote a continually decreasing angle between the magnetic field and the gravity vector. k denotes the time step. At time $k + 2$, the field resembles the magnetic equator.

scenarios could confer ecologically relevant capabilities. Moreover, the success of our stochastic model in completing full migrations highlights the potential usefulness of our method even when a migratory path is not direct (e.g. a bird being blown off course) or if sensitivity is substantially lower than discussed here.

Two previous studies have investigated mechanisms that might allow migratory birds to cross the magnetic equator [15,17]. This part of the migration is of particular interest because an avian magnetic strategy based on inclination cannot function when field lines are parallel to Earth's surface [16] and also because birds migrating south across the Equator must transition from moving 'equatorward' to moving 'poleward' [17]. In one study [17], birds (the Bobolink *Dolichonyx oryzivorus*) were tested in a planetarium under an unchanging star pattern while being exposed to a series of magnetic fields that the birds would encounter while migrating south across the Equator and into the Southern Hemisphere. Birds continued to orient in the appropriate southward direction throughout the experiment, suggesting that the experience of being in a field like that at the Equator, perhaps combined with stellar cues, enables them to transition to 'poleward' orientation after crossing the Equator and maintain consistent southward headings throughout the migration. A second study with the garden warbler (*Sylvia borin*) also suggests that exposure to a field like one at the magnetic equator was necessary for a bird to maintain orientation as it moves from the Northern Hemisphere to the Southern Hemisphere [15].

In our strategy, there is nothing particularly special about experience with the Equator. Instead, the agent only seeks a continually decreasing angle between the local magnetic field and gravity vectors. To see this, consider figure 8.

The top panel of figure 8 represents the progression of a real-world field, and the bottom represents an experimental manipulation, namely from [15]. If an animal tries to make the angle between the gravity vector and the local magnetic field continually decrease, then this would correspond to moving in the direction of the red arcs at each time step. In the top case, this would amount to continually moving in one direction (i.e. north or south), with successful motion across the Equator. In the bottom plots, this would correspond to a direction reversal, similar to the experimental observations of [15]. We emphasize here that our results do not mean or imply that an animal is necessarily using the strategy we have proposed, nor do they imply that animals do not require equatorial experience, prior migration experience, or other sensory cues to successfully navigate. Indeed, learning from experience is critically important for the survival of many animals, and the use of other sensory cues is likely at play in behaviours that involve magnetoreception (e.g. [62]). We are simply encouraged by the fact that our strategy, inspired by these previous animal experiments, generates results that are (i) consistent with the results of previous studies on navigation that leverage magnetic inclination, and (ii) may have applications in the development of new engineered navigation systems.

With respect to animal navigation, an interesting study would be to compare the model presented in this work with alternative implementations that require navigation experience, or multimodal sensing to navigate [15,17]. The present model and new models can be run under identical conditions to see when the results agree, and when disparities emerge, moving us closer to understanding how animals may use an inclination-based magnetic navigation system. We plan to execute this type of study in the future.

With respect to engineered navigation systems, it may be impractical for a system to have prior experience with the sensory environment. In this case, our strategy could be useful because it can work on a maiden voyage, though the ability of the system to learn online would be of great value and use. Also, engineered systems may have to be deployed for extended periods of time, or may only be deployed long after they are constructed. In both cases, the system must still satisfy a set of requirements, even if the sensory environment has changed over time. The results of our study suggest that an animal-inspired strategy may be able to tolerate these temporal changes, thus providing a potential bioinspired solution to an engineering problem [63].

It is interesting to note that there are both biological and engineered systems that execute tasks or take measurements in a sequential manner. For example, [10] describes birds that navigate to one area in Europe, then turn south, thereby migrating from Europe to Africa and avoiding major geographical barriers. Postlethwaite & Walker [31] model how sequential sensing in which there is a mismatch between a cognitive map and a real-world map might explain an initial orientation error that is experimentally observed in pigeons. Numerous engineered systems (e.g. Kalman filters) take and process measurements in a sequential manner [64]. It would be an interesting future work to examine the interplay between sequential behaviours, and information obtained from prior navigation experience.

The effectiveness of our model may be instructive for another open question in the study of magnetoreception: its

Downloaded from http://royalsocietypublishing.org/rsif/article-pdf/doi/10.1098/rsif.2020.0887/923617/rsif.2020.0887.pdf
by UNC Chapel Hill user
on 17 June 2026

evolution [65–67]. In general, sensory systems are thought to evolve in a piecewise manner, with each step conferring added fitness, as opposed to evolving de novo. For example, vision developed from non-directional photoreception [68]. However, it is harder to envision how a simple magnetic sense might have evolved into a system for guiding long-distance navigation [65]. Modelling by Taylor [69] demonstrated how a nervous system could use a basic magnetoreceptor to extract either single, or multiple features of the magnetic field. Here, we demonstrate the potential navigational utility of a simple magnetic sense that encodes a single aspect of the Earth's magnetic field. As such, our model may serve as a useful thought experiment when considering the evolutionary history of magnetic reception in animals.

Data accessibility. Code is provided as electronic supplementary material.

Authors' contributions. B.K.T. conceptualized the study, authored code and performed experiments, and was the primary author and contributor to the manuscript. K.J.L., L.T.H., C.M.F.L. and J.G. assisted with revising and editing the manuscript, and framing aspects of its direction. All authors contributed to various revisions of the paper.

Competing interests. We declare we have no competing interests.

Funding. This work was supported in part by a grant from the Air Force Office of Scientific Research (FA9550-20-1-0399), a fellowship from the National Defense Science and Engineering Graduate Fellowship Program, a fellowship from the National Science Foundation Graduate Research Fellowship Program, and internal grant funding from The University of North Carolina at Chapel Hill.

Acknowledgements. The authors thank Kayla Goforth for her critique of the work, and J.R. Elliott for generating the world magnetic map image.

Appendix A

(a) Motion model

Velocity in spherical coordinates is given as

$$\vec{v}_{\text{sph}} = \begin{bmatrix} v_{\text{radial}} \\ v_{\text{meridian}} \\ v_{\text{polar}} \end{bmatrix} = \begin{bmatrix} \dot{\rho} \\ \rho\dot{\phi} \\ \rho\dot{\theta}\sin(\phi) \end{bmatrix} \tag{A 1}$$

The following updates the Cartesian position given a spherical coordinate velocity and position

$$\vec{x}_{k+1} = \vec{x}_k + \begin{bmatrix} c\theta s\phi & c\theta c\phi & -s\theta \\ s\theta s\phi & s\theta c\phi & c\theta \\ c\phi & s\phi & 0 \end{bmatrix}_k \vec{v}_{\text{sph}}\,\Delta t, \tag{A 2}$$

where the matrix in equation (A 2) expresses vectors from the spherical (rotating) frame in a fixed XYZ frame, k is the current time step, and $k+1$ is the next time step.

(b) Inclination calculation

To compute the standard definition of inclination from our definition, we can use the point slope formula with α, and λ, or,

$$\alpha = \left(\frac{\alpha_2 - \alpha_1}{\lambda_2 - \lambda_1}\right)(\lambda - \lambda_1) + \alpha. \tag{A 3}$$

Looking at figure 4, we can see that at the North Pole, $\lambda = 0°$, and at the Equator, $\lambda = -90°$. From the standard definition, $\alpha = 90°$ at the North Pole, and 0° at the Equator. Plugging these values in and simplifying give the following:

$$\alpha = -\lambda - 90 \tag{A 4}$$

(c) Stochastic calculation

Mathematically, $\dot{\phi}$ is computed the following way in the stochastic scenario

$$\dot{\phi}_k = \dot{\phi}_{k-1} + \eta f(j), \tag{A 5}$$

where

$$f(j) = \begin{cases} 0 & 0 \le j < j_1 \\ \frac{1}{j_2 - j_1}(j - j_1) & j_1 \le j \le j_2 \\ 1 & j_2 < j \end{cases} \tag{A 6}$$

and

$$\eta = \mathcal{N}(\mu = 0, \sigma^2 = \sigma_\eta^2); \quad j_1 = 5; \quad j_2 = 8.$$

In these equations, j is the number of time steps that have elapsed since a measurement was last taken, while k is the current time step. Equation (A 5) has the effect of setting the angular velocity $\dot{\phi}_j$ to its value at the previous time step, plus a noise value that starts at zero and steadily increases over time in a piece-wise linear manner. For this study, $\sigma_\eta = 10°$.

References

1. Shockley JA, Raquet JF. 2014 Navigation of ground vehicles using magnetic field variations. *Navigation* **61**, 237–252. (doi:10.1002/navi.70)
2. Canciani A, Raquet JF. 2016 Absolute positioning using the Earth's magnetic anomaly field. *Navigation* **63**, 111–126. (doi:10.1002/navi.138)
3. Johnsen S, Lohmann KJ. 2005 The physics and neurobiology of magnetoreception. *Nat. Rev. Neurosci.* **6**, 703–712. (doi:10.1038/nrn1745)
4. Johnsen S, Lohmann KJ. 2008 Magnetoreception in animals. *Phys. Today* **61**, 29–35. (doi:10.1063/1.2897947)
5. Wiltschko R, Wiltschko W. 1995 *Magnetic orientation in animals*. Berlin Heidelberg, Germany: Springer.
6. Knecht DJ, Shuman BM. 1985 The geomagnetic field. In *Handbook of geophysics and the space environment* (ed. A Jursa). Springvale, VA: Air Force Geophysics Laboratory.
7. Wajnberg E, Acosta-Avalos D, Alves OC, de Oliveria JF, Srygley RB, Esquivel DMS. 2010 Magnetoreception in eusocial insects: an update. *J. R. Soc. Interface* **7**, S207–S225. (doi:10.1098/rsif.2009.0526.focus)
8. Huang G, Taylor BK, Akopian D. 2019 A low-cost approach of magnetic field-based location validation for global navigation satellite systems. *IEEE Trans. Instrum. Meas.* **68**, 4937–4944. (doi:10.1109/TIM.2019.2901512)
9. Lohmann KJ, Hester JT, Lohmann CMF. 1999 Long-distance navigation in sea turtles. *Ethol. Ecol. Evol.* **11**, 1–23. (doi:10.1080/08927014.1999.9522838)
10. Lohmann KJ, Lohmann CMF, Putman NF. 2007 Magnetic maps in animals: nature's GPS. *J. Exp. Biol.* **210**, 3697–3705. (doi:10.1242/jeb.001313)
11. Lohmann KJ, Putman NF, Lohmann CMF. 2012 The magnetic map of hatchling loggerhead sea turtles. *Curr. Opin Neurobiol.* **22**, 336–342. (doi:10.1016/j.conb.2011.11.005)
12. Reppert SM, Gegear RJ, Merlin C. 2010 Navigational mechanisms of migrating monarch butterflies. *Trends Neurosci.* **33**, 399–406. (doi:10.1016/j.tins.2010.04.004)
13. Dreyer D, Frost B, Mouritsen H, Günther A, Green K, Whitehouse M, Johnsen S, Heinze S, Warrant E. 2018 The Earth's magnetic field and visual landmarks steer migratory flight behavior in the nocturnal Australian bogong moth. *Curr. Biol.* **28**, 2160–2166.e2165. (doi:10.1016/j.cub.2018.05.030)
14. Wiltschko W, Munro U, Ford H, Wiltschko R. 1993 Magnetic inclination compass: a basis for the migratory orientation of birds in the Northern and Southern Hemisphere. *Experientia* **49**, 167–170. (doi:10.1007/BF01989423)
15. Wiltschko W, Wiltschko R. 1992 Migratory orientation: magnetic compass orientation of

Downloaded from http://royalsocietypublishing.org/rsif/article-pdf/doi/10.1098/rsif.2020.0887/923617/rsif.2020.0887.pdf
by UNC Chapel Hill user
on 17 June 2026

garden warblers (*Sylvia borin*) after a simulated crossing of the magnetic equator. *Ethology* **91**, 70–74. (doi:10.1111/j.1439-0310.1992.tb00851.x)

16. Wiltschko W, Wiltschko R. 1972 Magnetic compass of european robins. *Science* **176**, 62–64. (doi:10.1126/science.176.4030.62)
17. Beason RC. 1992 You can get there from here: responses to simulated magnetic equator crossing by the bobolink (*Dolichonyx oryzivorus*). *Ethology* **91**, 75–80. (doi:10.1111/j.1439-0310.1992.tb00852.x)
18. Jensen KK. 2010 Light-dependent orientation responses in animals can be explained by a model of compass cue integration. *J. Theor. Biol.* **262**, 129–141. (doi:10.1016/j.jtbi.2009.09.005)
19. Johnsen S, Lohmann KJ, Warrant EJ. 2020 Animal navigation: a noisy magnetic sense? *J. Exp. Biol.* **223**, jeb164921. (doi:10.1242/jeb.164921)
20. Putman NF. 2015 Inherited magnetic maps in salmon and the role of geomagnetic change. *Integr. Comp. Biol.* **55**, 396–405. (doi:10.1093/icb/icv020)
21. Hiscock HG, Mouritsen H, Manoloupoulos DE, Hore PJ. 2017 Disruption of magnetic compass orientation in migratory birds by radiofrequency electromagnetic fields. *Biophys. J.* **113**, 1475–1484. (doi:10.1016/j.bpj.2017.07.031)
22. Hore PJ, Mouritsen H. 2016 The radical-pair mechanism of magnetoreception. *Annu. Rev. Biophys.* **45**, 299–344. (doi:10.1146/annurev-biophys-032116-094545)
23. Vidal-Gadea A *et al.* 2015 Magnetosensitive neruons mediate geomagnetic orientation in *Caenorhabditis elgans*. *eLife* **4**, e07493. (doi:10.7554/eLife.07493)
24. Shaw J, Boyd A, House M, Woodward R, Falko M, Cowin G, Saunders M, Baer B. 2015 Magnetic particle-mediated magnetoreception. *J. R. Soc. Interface* **12**, 20150499. (doi:10.1098/rsif.2015.0499)
25. Treiber CD *et al.* 2012 Clusters of iron-rich cells in the upper beak of pigeons are macrophages not magnetosensitive neurons. *Nature* **484**, 367–370. (doi:10.1038/nature11046)
26. Eder SHK, Cadiou H, Muhamad A, McNaughton PA, Kirschvink JL, Winklhofer M. 2012 Magnetic characterization of isolated candidate vertebrate magnetoreceptor cells. *Proc. Natl Acad. Sci. USA* **109**, 12 022–12 027. (doi:10.1073/pnas.1205653109)
27. Edelman NB *et al.* 2015 No evidence for intracellurlar magnetite in putative vertebrate magnetoreceptors identified by magnetic screeneing. *Proc. Natl Acad. Sci. USA* **112**, 262–267. (doi:10.1073/pnas.1407915112)
28. Lohmann KJ. 2010 Magnetic-field perception. *Nature* **464**, 1140–1142. (doi:10.1038/4641140a)
29. Painter KJ, Hillen T. 2015 Navigating the flow: individual and continuum models for homing in flowing environments. *J. R. Soc. Interface* **12**, 20150647. (doi:10.1098/rsif.2015.0647)
30. Painter KJ, Plochocka AZ. 2019 Efficiency of island homing by sea turtles under multimodal navigating strategies. *Ecol. Modell* **391**, 40–52. (doi:10.1016/j.ecolmodel.2018.10.025)
31. Postlethwaite CM, Walker MM. 2011 A gemoetric model for initial orientation errors in pigeon navigation. *J. Theor. Biol.* **269**, 273–279. (doi:10.1016/j.jtbi.2010.10.036)
32. Benhamou S. 2003 Bicoordinate navigation based on non-orthogonal gradient fields. *J. Theor. Biol.* **225**, 235–239. (doi:10.1016/S0022-5193(03)00242-X)
33. Taylor BK. 2017 Bioinspired magnetic reception and multimodal sensing. *Biol. Cybern* **111**, 287–308. (doi:10.1007/s00422-017-0720-3)
34. Taylor BK. 2018 Bioinspired magnetoreception and navigation using magnetic signatures as waypoints. *Bioinspir. Biomim.* **13**, 046003. (doi:10.1088/1748-3190/aabbec)
35. Taylor BK, Corbin S. 2019 Bioinspired magnetoreception and navigation in nonorthogonal environments using magnetic signatures. *Bioinspir. Biomim.* **14**, 066009. (doi:10.1088/1748-3190/ab40f8)
36. Putman NF, Verley P, Shay TJ, Lohmann KJ. 2012 Simulating transoceanic migrations of young loggerhead sea turtles: merging magnetic navigation behavior with an ocean circulation model. *J. Exp. Biol.* **215**, 1863–1870. (doi:10.1242/jeb.067587)
37. Putman NF, Verley P, Endres CS, Lohmann KJ. 2015 Magnetic navigation behavior and the oceanic ecology of young loggerhead sea turtles. *J. Exp. Biol.* **218**, 1044–1050. (doi:10.1242/jeb.109975)
38. Rutter BL, Taylor BK, Bender JA, Blűmel MA, Lewinger WA, Ritzmann RE, Quinn RD. 2011 Descending commands to an insect leg controller network cause smooth behavioral transitions. In *Proc. of the IEEE Int. Conf. on Intelligent Robots and Systems, San Francisco, CA, 25–30 September*, pp. 215–220. New York, NY: IEEE.
39. Rutter BL, Taylor BK, Bender JA, Blűmel MA, Lewinger WA, Ritzmann RE, Quinn RD. 2011 Sensory coupled action switching modules (SCASM) for modeling and synthesis of biologically inspired coordination. In *Field Robotics: Proc. of the 14th Int. Conf. On Climbing and Walking Robots and the Support Technologies For Mobile Machines, CLAWAR 2011*, pp. 196–203. Singapore: World Scientific Publishing.
40. Szczecinski NS, Hunt AJ, Quinn RD. 2017 Design process and tools for dynamic neuromechanical models and robot controllers. *Biol. Cybern.* **111**, 105–127. (doi:10.1007/s00422-017-0711-4)
41. Szczecinski NS, Getsy AP, Martin JP, Ritzmann RE, Quinn RD. 2017 Mantisbot is a robotic model of visually guided motion in the praying mantis. *Arthropod Struct. Dev.* **46**, 736–751. (doi:10.1016/j.asd.2017.03.001)
42. Shi RZ, Horiuchi TK. 2007 A neuromorphic VLSI model of bat interaural level difference processing for azimuthal echolocation. *IEEE Trans. Circuits Syst. I* **54**, 74–88. (doi:10.1109/TCSI.2006.887981)
43. Grasso FW, Consi TR, Mountain DC, Atema J. 2000 Biomimetic robot lobster performs chemo-orientation in turbulence using an pair of spatially separated sensors: progress and challenges. *Robot. Auton. Syst.* **30**, 115–131. (doi:10.1016/S0921-8890(99)00068-8)
44. Grasso FW, Atema J. 2002 Integration of flow and chemical sensing for guidance of autonomous marine robots in turbulent flows. *Environ. Fluid Mech.* **2**, 95–114. (doi:10.1023/A:1016275516949)
45. Lohmann K, Pentcheff N, Nevitt G, Stetten G, Zimmer-Faust R, Jarrard H, Boles LC. 1995 Magnetic orientation of spiny lobsters in the ocean: experiments with undersea coil systems. *J. Exp. Biol.* **198**, 2041–2048.
46. Hedd A, Montevecchi WA, Otley H, Phillips RA, Fifield DA. 2012 Trans-equatorial migration and habitat use by sooty shearwaters *Puffinus griseus* from the South Atlantic during the nonbreeding season. *Mar. Ecol. Progress Ser.* **449**, 277–290. (doi:10.3354/meps09538)
47. Skomal GB, Zeeman SI, Chisholm JH, Summers EL, Walsh HJ, McMahon KW, Thorrold SR. 2009 Transequatorial migrations by basking sharks in the western Atlantic Ocean. *Curr. Biol.* **19**, 1019–1022. (doi:10.1016/j.cub.2009.04.019)
48. Rizzo Ly, Schulte D. 2009 A review of humpback whales' migration patterns worldwide and their consequences to gene flow. *J. Mar. Biol. Assoc. UK* **89**, 995–1002. (doi:10.1017/S0025315409000332)
49. Mellone U, López-López P, Limiñana R, Piasevoli G, Urios V. 2013 The trans-equatorial loop migration system of Eleonora's falcon: differences in migration patterns between age classes, regions and seasons. *J. Avian Biol.* **44**, 417–426. (doi:10.1111/j.1600-048X.2013.00139.x)
50. Møller PR, Nielsen JG, Fossen I. 2003 Patagonian toothfish found off Greenland. *Nature* **421**, 599–599. (doi:10.1038/421599a)
51. Egevang C, Stenhouse IJ, Phillips RA, Petersen A, Fox JW, Silk JR. 2010 Tracking of Arctic terns *Sterna paradisaea* reveals longest animal migration. *Proc. Natl Acad. Sci. USA* **107**, 2078–2081. (doi:10.1073/pnas.0909493107)
52. Leonhardt R, Fabian K. 2007 Paleomagnetic reconstruction of the global geomagnetic field evolution during the Matuyama/Brunhes transition: iterative Bayesian inversion and independent verification. *Earth Planet. Sci. Lett.* **253**, 172–195. (doi:10.1016/j.epsl.2006.10.025)
53. Sagnotti L, Scardia G, Giaccio B, Liddicoat JC, Nomade S, Renne PR, Sprain CJ. 2014 Extremely rapid directional change during Matuyama-Brunhes geomagnetic polarity reversal. *Geophys. J. Int.* **199**, 1110–1124. (doi:10.1093/gji/ggu287)
54. Ginsberg J. 2008 *Engineering dynamics*. New York, NY: Cambridge University Press.
55. Stevens BL, Lewis FL. 2003 *Aircraft control and simulation*. New York, NY: John Wiley and Sons.
56. Wilson H. 1999 *Spikes, decisions, and actions: the dynamical foundations of neuroscience*. Oxford, UK: Oxford University Press.
57. Boström JE, Akesson S, Alerstam T. 2012 Where on Earth can animals use a geomagnetic bi-coordinate map for navigation? *Ecography* **35**, 1039–1047. (doi:10.1111/j.1600-0587.2012.07507.x)
58. Lohmann KJ, Lohmann CMF. 2019 There and back again: natal homing by magnetic navigation in sea

Downloaded from http://royalsocietypublishing.org/rsif/article-pdf/doi/10.1098/rsif.2020.0887/923617/rsif.2020.0887.pdf
by UNC Chapel Hill user
on 17 June 2026

turtles and salmon. *J. Exp. Biol.* **222**(Suppl. 1), jeb184077. (doi:10.1242/jeb.184077)
59. Wynn J, Padget O, Mouritsen H, Perrins C, Guilford T. 2020 Natal imprinting to the Earth's magnetic field in a pelagic seabird. *Curr. Biol.* **30**, 2869–2873. (doi:10.1016/j.cub.2020.05.039)
60. Pennycuick CJ, Akesson S, Hedenstrom A. 2013 Air speeds of migrating birds observed by ornithodolite and compared with predictions from flight theory. *J. R. Soc. Interface* **10**, 20130419. (doi:10.1098/rsif.2013.0419)
61. Kralj J, Martinovic M, Jurinovic L, Szinai P, Süto S, Preiszner B. 2020 Geolocator study reveals east African migration route of Central European common terns. *Avian Res.* **11**, 6. (doi:10.1186/s40657-020-00191-z)
62. Endres CS, Putman NF, Ernst DA, Kurth JA, Lohmann CMF, Lohmann KJ. 2016 Multi-modal homing in sea turtles: modeling dual use of geomagnetic and chemical cues in island-finding. *Front. Behav. Neurosci.* **10**, 19. (doi:10.3389/fnbeh.2016.00019)
63. Lepora NF, Verschure P, Prescott TJ. 2012 The state of the art in biomimetics. *Bioinspir. Biomim.* **8**, 013001. (doi:10.1088/1748-3182/8/1/013001)
64. Crassidis JL, Junkins JL. 2012 *Optimal estimation of dynamic systems*. Boca Raton, FL: CRC Press.
65. Gould JL. 2008 Animal navigation: the evolution of magnetic orientation. *Curr. Biol.* **18**, R482–R484. (doi:10.1016/j.cub.2008.03.052)
66. Occhipinti A, De Santis A, Maffei ME. 2013 Magnetoreception: an unavoidable step for plant evolution? *Trends Plant Sci.* **19**, 1–4. (doi:10.1016/j.tplants.2013.10.007)
67. Lin W, Kirschvink JL, Paterson GA, Bazylinski DA, Yongxin P. 2020 On the origin of microbial magnetoreception. *Natl Sci. Rev.* **7**, 472–479. (doi:10.1093/nsr/nwz065)
68. Land MF, Nilsson D-E. 2002 *Animal eyes*. Oxford, UK: Oxford University Press. (doi:10.1093/acprof:oso/9780199581139.001.0001)
69. Taylor BK. 2016 Validating a model for detecting magnetic field intensity using dynamic neural fields. *J. Theor. Biol.* **408**, 53–65. (doi:10.1016/j.jtbi.2016.08.010)

Downloaded from http://royalsocietypublishing.org/rsif/article-pdf/doi/10.1098/rsif.2020.0887/923617/rsif.2020.0887.pdf
by UNC Chapel Hill user
on 17 June 2026